HUNGARIAN JOURNAL
OF INDUSTRIAL CHEMISTRY
VESZPRÉM
Vol. 39(1) pp. 141-146 (2011)

ANALYSIS AND MODELING OF SLOTLESS PERMANENT MAGNET SYNCHRONOUS MOTORS

I. SZALAY[1✉], H. MEDVE, D. FODOR[2✉]

University of Pannonia, Institute of Mechanical Engineering, Automotive System Engineering Group
8200 Veszprém, Egyetem u. 10, HUNGARY
[1✉]E-mail: ifj.szalay.istvan@gmail.com
[2✉]E-mail: fodor@almos.uni-pannon.hu

In the automotive industry, where reliability and cost efficiency are especially important, applications based on permanent magnet synchronous motors are gaining more and more ground. The slotless PMSMs have high power and torque density, but they are much more difficult to model than iron cored ones and their sensorless control has not yet been completely solved. The main aims of this study are to better understand the physical phenomena in a slotless PMSM caused by the high frequency injection at standstill, to present an automated measurement environment and measurement results, and to suggest a partial position detection method for slotless PMSMs at standstill.

Keywords: slotless permanent magnet synchronous motor, air core winding, modelling, sensorless position detection, initial position detection, high frequency injection, digital signal processing.

Introduction

Sensorless control of Permanent Magnet Synchronous Motors is a low cost and reliable alternative to traditional sensor based PMSM control and therefore is becoming widely accepted by the industry. During the latest decades various sensorless methods has been developed, which can be used successfully in the control of conventional variants of PMSMs.

The control of PMSMs is based on the rotor position feedback, which is essential to perform correctly the electronic commutation. To start the motor without any unwanted vibration and reverse rotation, as it is required in many applications, and to do precise position control, it is necessary to know the initial rotor position. However, there are some types of PMSMs, such as slotless ones, on which the standard sensorless position detection methods fail at low and zero speed or behave in unpredictable ways at any speed, making it impossible to detect the initial rotor position.

The most promising sensorless method for precise initial position detection is high frequency signal injection, which is able to transform the effect of anisotropic characteristics of $Nd_2Fe_{14}B$ permanent magnet rotor into angle dependent electrical quantities. This means that the (current, induced voltage, etc.) response of the PMSM for a given sinusoidal excitation voltage will vary, depending on the rotor position. The high frequency signal injection can be used with slotless air-core winding motors too, because the success of the measurement depends on the anisotropic properties of the permanent magnet instead iron saturation.

In this study, the analysis of slotless PMSMs is presented including mathematical and physical modelling of the rotor permanent magnet and a differential measurement method of the induced voltages at zero speed. Measurement result, signal plots, a National Instruments LabVIEW[1] based automated measurement environment, the discovered motor characteristics and based on these motor characteristics, a partial sensorless rotor position detection method for slotless PMSMs are also presented with explanations and comments on them.

Mathematical modelling

Electric drives are complex electromechanical systems. Their power supply and their control is usually electrical and their output is usually mechanical. Therefore usually their modeling is interested in only the electrical and mechanical phenomena. However, if the magnetic structure of the motor is important (because the existence of anisotropies, saturation, hysteresis, and the combination of them are not negligible) then it should be taken into consideration thoroughly.

Most of sensorless position detection methods are based on the anisotropic magnetic phenomena, so the analysis of the magnetic structure and its effect on the electrical signal is very important from both theoretical and experimental view.

[1] LabVIEW is a trademark of National Instruments Corporation

Geometric model

The modeled PMSMs are cylindrically designed ones, they have 3 phase slotless windings on their stator and a cylindrical permanent magnet on their rotor (see *Fig. 1*).

The motor parts are considered to be perfectly cylindrical shaped.

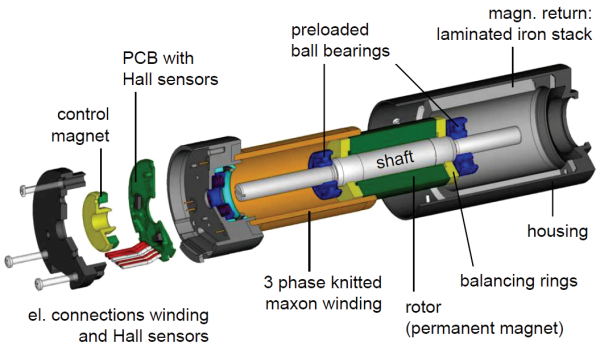

Figure 1: The tructure of a slotless PMSM

Electrical model

The voltage equations of the phases (the voltage reference point is the star point):

$$U_i = \frac{d\Phi_i}{dt} + Ri_i \qquad (1)$$

where:

U_i, i_i – voltage and current of Phase i

Φ_i – magnetic flux in Phase i

R – resistance of one phase winding

The flux in Phase i can be dissolved into flux components that are produced by the windings and the permanent magnet:

$$U_i = \frac{d}{dt}\left(\Phi_{ia} + \Phi_{ib} + \Phi_{ic} + \Phi_{Mi}\right) + Ri_i \qquad (2)$$

where:

Φ_{ij} – magnetic flux component in Phase i produced by Phase j

Φ_{Mi} – magnetic flux component in Phase i produced by the permanent magnet rotor

The phase flux can be dissolved into products of inductances and current derivatives:

$$\Phi_i = L_{ia}i_a + L_{ib}i_b + L_{ic}i_c + \Phi_{Mi} \qquad (3)$$

where:

L_{ia}, L_{ib}, L_{ic} – inductances corresponding to Phase i

The change of the phase flux component from the permanent magnet induces the following voltage component, which can be considered proportional to the actual rotor angular speed, so the flux of the permanent magnet is constant, only rotation can cause changes.

Equation (3) defines three flux equations for a three phase motor. The vectorial flux equation, which describes the relation between the phase fluxes and phase currents:

$$\begin{bmatrix}\Phi_a\\ \Phi_b\\ \Phi_c\end{bmatrix} = \frac{1}{N}\begin{bmatrix}L_{aa} & L_{ab} & L_{ac}\\ L_{ba} & L_{bb} & L_{bc}\\ L_{ca} & L_{cb} & L_{cc}\end{bmatrix}\begin{bmatrix}i_a\\ i_b\\ i_c\end{bmatrix} + \begin{bmatrix}\Phi_{Ma}\\ \Phi_{Mb}\\ \Phi_{Mc}\end{bmatrix} \qquad (4)$$

$$\underline{\Phi} = \frac{1}{N}\underline{\underline{L}}\underline{i} + \underline{\Phi}_M \qquad (5)$$

where:

$\underline{\Phi}$, $\underline{\Phi}_M$ – total and permanent magnet flux vectors

$\underline{\underline{L}}$ – inductance matrix

N – number of turns of a phase winding

In the development of the sensorless method's mathematical background it is an important task to determine the $\underline{\underline{L}}$ inductance matrix, and its dependencies on the other physical quantities, especially the rotor's angular position. In the magnetic modeling one of the main goals will be to write the inductance matrix into a form, which uses the magnetic properties of the motor.

The inductance matrix is important also because it is the mathematical object which describes the relationship between the electric and magnetic parts of the model.

Magnetic model

The most important physical phenomena were the followings during the mathematical modeling of the motor's magnetic structure:

Saturation: The rotor permanent magnets reluctance is flux dependent.

Hysteresis: B-H curve of a permanent magnet is a hysteresis loop.

Anisotropies: The rotor permanent magnets reluctance and probably the saturation and the hysteresis are anisotropic quantities. Another phenomenon, that should be considered, is the eddy current on the rotor permanent magnet surface. For geometrical reason the motor model should be divided into two parts: stator and air gap model, rotor model.

Stator and air gap: Stator contains the air core windings, the air gap between the windings and the rotor, and the external iron cylinder. The air gap and the air core can be discussed together as a simple reluctance. The external iron cylinder, the air core and the air gap can be modeled as constant reluctances. The stator windings are magnetomotive forces in the magnetic circuit.

Rotor: The rotor is a permanent magnet, which is a cylinder-shaped object. The permanent magnet can be modeled as a magnetic circuit, which contains reluctances and magnetomotive forces. First it is practical to model separately the reluctances and the magnetomotive forces, to create a reluctance model and a magnetomotive model, and then connect them. Suppose the rotor is cylindrical perfectly, the magnetic field of the rotor permanent magnet is symmetrical to the plane defined by the *d* axis and motor shaft.

The field lines of the magnetic field go through the rotor surface only on the cylinder-cover. The flux flowing through the cylinder base of the rotor is zero. The field lines don't close inside the rotor permanent magnet, so the leakage flux is 0 Wb.

Reluctance model

Hypothesis: The reluctance between two circumferential points opposite each other depends on the point pair and the flux flowing from one to the other. In other words, using the symbols of *Fig. 2*, the reluctance $\Re_{AB}$ depends on the angle φ_1 and $\Re_{CD}$ depends on φ_3 and both reluctances depend on the actual Φ flux flowing through the permanent-magnet.

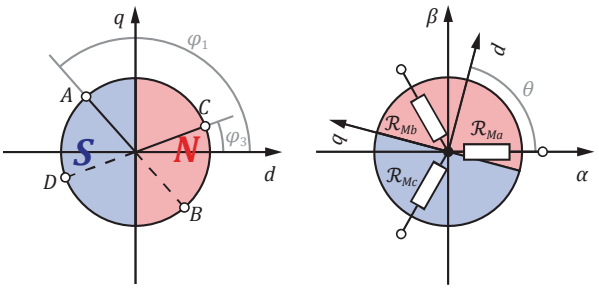

Figure 2: Illustration of reluctancies between arbitrary circumferential points (left) and the equivalent star connected reluctances (right)

So any φ angle and Φ flux define an $\Re(\varphi, \Phi)$ "passing through" reluctance value, which can be divided into two radial reluctance components:

$$\Re(\varphi_1, \Phi) = \Re_M(\varphi_1, \Phi) + \Re_M(\varphi_1 + \pi, -\Phi) \qquad (6)$$

where $\Re_M(\varphi, \Phi)$ is the "radial" reluctance function of the rotor magnet, which defines the "radial" reluctance between the center and the surface point in the direction of the φ angle, when the flux flowing through is Φ.

The reluctance between non-opposite surface points can be divided into two "radial" reluctances. For example, the reluctance between the points A and C, when Φ flux flowing through from point A to point C, is computed in the following way using the $\Re_M(\varphi, \Phi)$ function:

$$\Re_{AC} = \Re_M(\varphi_1, \Phi) + \Re_M(\varphi_3, -\Phi) \qquad (7)$$

where:

φ_1, φ_3 – see Fig. 2.

The above method has some error, which is greater when the difference of the two angles (in the above example the difference of φ_1 and φ_2) is smaller. If the difference is large enough (for example 120°, as it is between the center lines of the phase windings), then the error can be acceptable.

The whole rotor magnet can be modeled as reluctances connected in a star using the $\Re_M(\varphi, \Phi)$ function, see Fig. 2 (right). The phase reluctances and their pins are fixed in the standing coordinate system. Because the rotor can rotate, the value of the phase reluctances will change, and will depend on the rotor position θ. Describing the phase reluctances with the $\Re_M(\varphi, \Phi)$ function yields with indexed quantities:

$$\Re_{Mi} = \Re_M\left(-\theta + i\frac{2\pi}{3}, \Phi_i\right) \qquad (8)$$

where $\Re_{Mi}$ is the reluctance component of phase i at θ angular rotor position.

Magnetomotive model

The flux density by the circumference is supposed to be sinusoidal. *Fig. 3* shows flux density is plotted against the φ angle in the $(d - q)$ coordinate system.

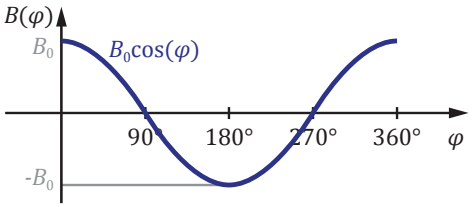

Figure 3: Flux density by the circumference

The flux density by the circumference is supposed to be sinusoidal. Suppose the flux density is parallel to the surface normal in every point of the surface.

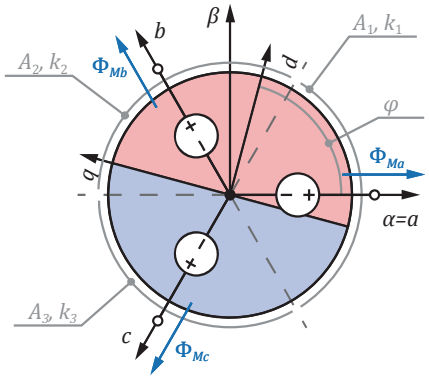

Figure 4: The magnetomotive forces, reduced into three parts and three pins

The rotor's model should have three pins for connect them to the three phases through the air gaps. These pins are surface third parts contracted into single points. The pins are on the centers of the third parts which are 120° parts of the cylinder-cover.

The fluxes flowing through the surface third parts, which are attached to the fixed (α – β) system, depends on the θ angular rotor position.

Measurement conception

In the focus of the performed measurements was the data acquisition for developing the high frequency injection based sensorless rotor position detection method of the PMSMs at zero speed. The analysis of the rotor position's effect on the induction, induced voltages, and current response requires measurement data.

The examined motors were a Maxon EC 118890 with two pole rotor magnet and a Maxon 252463 type motor with four pole rotor magnet.

Excitation process

On the examined motors one phase excitation method has been applied using the star points of them. In the automated process the stepper motor (48 steps per rotations) rotates the rotor of the PMSM to the desired position. The connection of the non-excited windings to the oscilloscope and the excited winding to the amplified function generator output is provided by the control strategy of relay network. This procedure is repeated for all three phases of the motor, so this method results in three measurements at a specified angular position.

The three phase voltages are treated as excitation voltage (U_e), "positive" induced voltage (U_p) and "negative" induced voltage (U_n). The "positive" and "negative" denominations are for clearing the sign of the ΔU difference.

In the performed measurements the amplitude of the excitation voltage was 5 V, the frequency was 1 kHz.

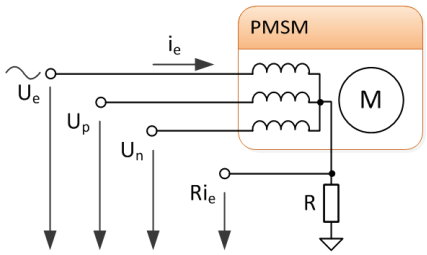

Figure 5: The measurement configuration and the measured signals. The star point of the stator winding has been made accessible for measurement purposes

Table 1: Excitation and measurement pattern

U_e (excited)	U_p (meas.)	U_n (meas.)	$\Delta U=U_p-U_n$
1	2	3	2-3
2	3	1	3-1
3	1	2	1-2

Table 1 defines the roles of the phase windings during the three steps of the measurement at a specified position, and the definition of the induced voltage difference, ΔU.

Measurement environment

The measurement environment includes a Tektronix® MSO4154B oscilloscope, a Tektronix® AFG3022B arbitrary function generator, and a control card for isolation, switching and stepper driving purposes. Data acquisition and high level control is performed by National Instruments LabVIEW (see *Fig. 6*).

The measurable physical quantities:

- Excitation voltage before or after amplifying,
- Current response in the excited phase winding,
- Induced voltages in the non-excited phase windings,
- Difference of the induced voltages, amplified by an instrumentation amplifier

The measurements have been done by 1 µs sample time, which was enough to sample 1 kHz frequency signals without aliasing.

The waveform, amplitude and frequency of the excitation voltage are automatically adjustable. The simplest way of high frequency current measurement was the use of a precision current shunt.

Measurement results

Measurements from 0° to 360° with 48 step resolution has been performed to get the entire angular characteristics of the induced voltage difference. The results of the measurements can be seen on *Fig. 7* and *Fig. 8*.

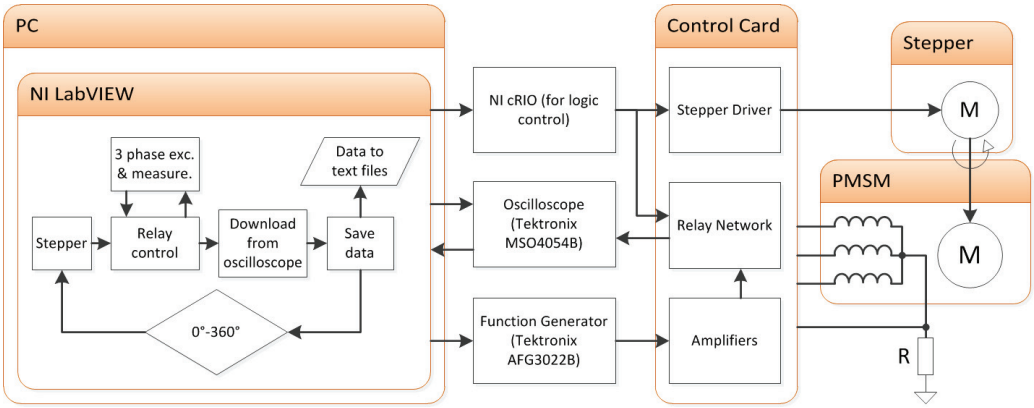

Figure 6: Structure of the measurement automation environment

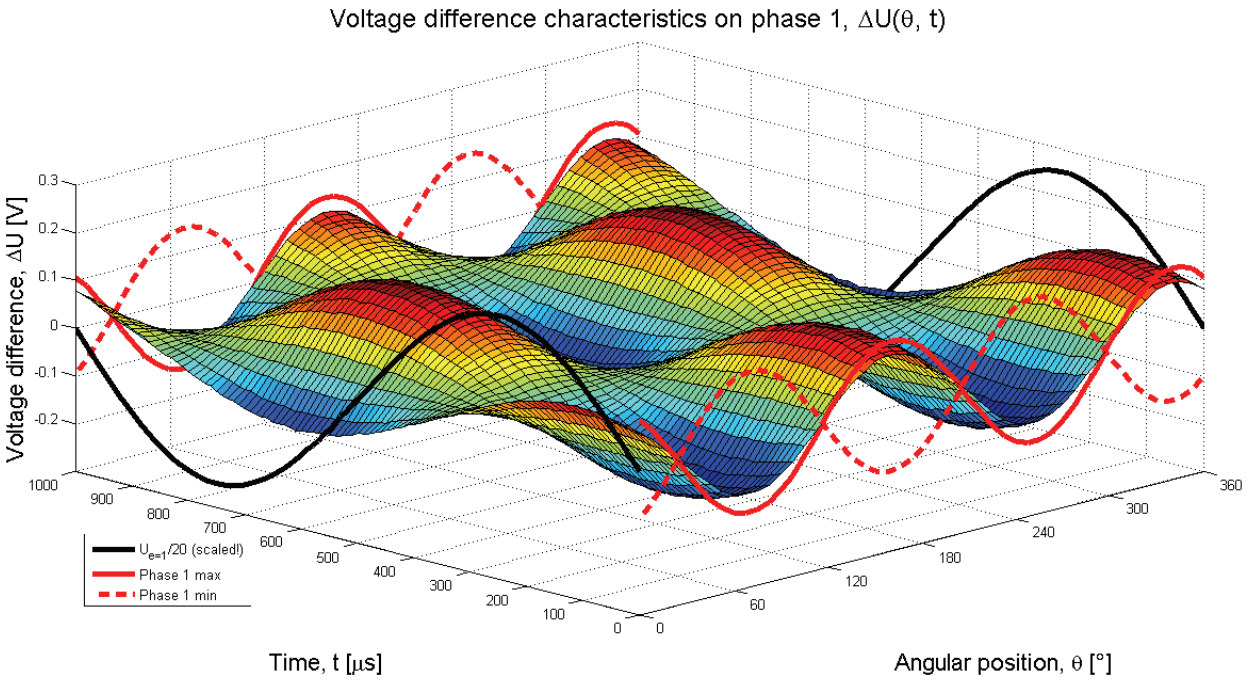

Figure 7: The characteristics of the measured induced voltage difference on the Maxon EC 118890 while phase 1 was excited (coloured 3D surface, z(x, y) = $\Delta U(\theta, t)$), the scaled excitation voltage (black line, for phase illustration) and the extreme values of the difference signal (red lines).

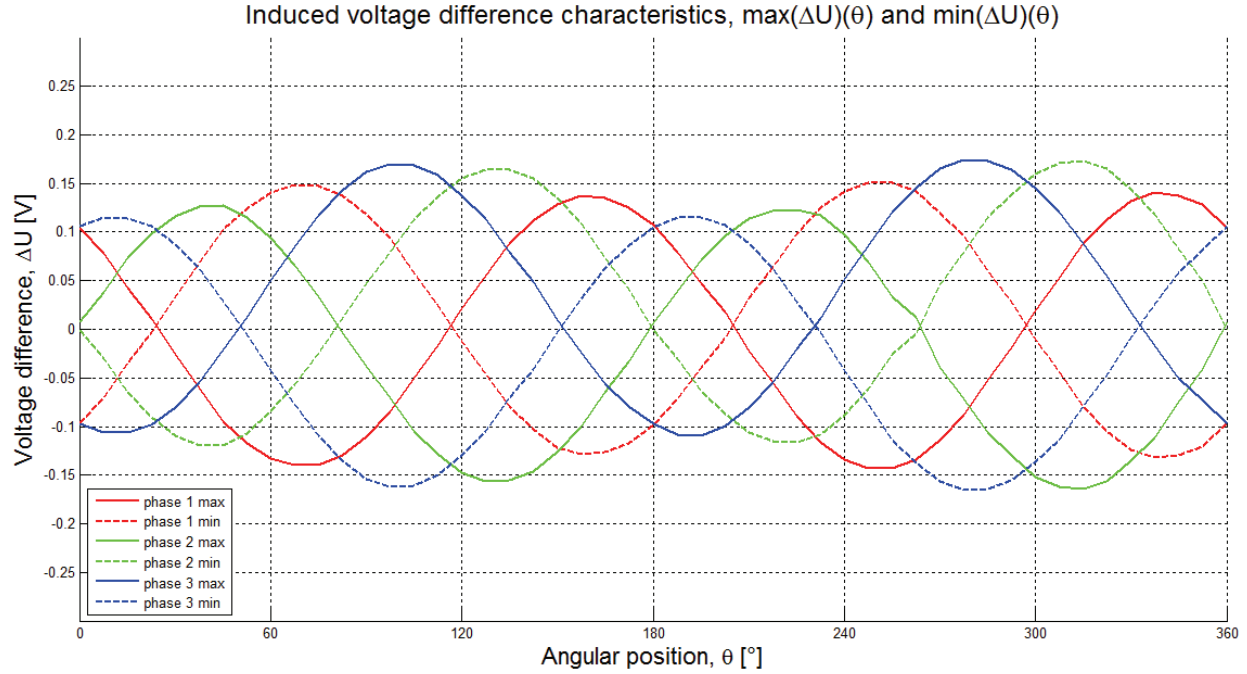

Figure 8: The induced voltage difference characteristics for all the three phases. Continuous lines show the extreme values of differences closer to the maximum of the corresponding excitation voltage, dashed lines show the closer to the minimum

Characteristic curves shown on Fig. 7 and Fig. 8 prove the existence of measurable anisotropic effect of the permanent magnet on the electrical signal, in the case of slotless Maxon PMSMs. In the case of 5 V excitation voltages, the difference between the induced voltages reaches the 100–180 mV interval, depending on the excited phase.

The weakness of the discovered phenomenon has a periodicity of 180° (all the curves on Fig. 8 have a periodicity of 180°), which isn't enough to clearly determine the rotor position; the number of possible rotor position values can be reduced to two opposite angular position (0 – π ambiguity problem).

Data analysis

The primary goal of the data analysis is to find the anisotropic characteristics – angular dependencies of electric parameters and signals – of the Maxon slotless PMSMs. Simplest way of anisotropy analysis is the construction of the characteristics of a measured or computed quantity versus angular position. MathWorks® MATLAB®[2] has been chosen as development environment for signal analysis and data visualization. A processing program has been developed, which visualize the excitation voltage and current, the induced voltages and their difference, the phase shift between any of the chosen signals, amplitude characteristics, phase characteristics, inductivity changes.

The processing program reads the signals from the text files generated by the selected measurement, and performs some preprocessing and signal conditioning task, like filtering, amplification and scaling.

Induced voltage difference analysis

Fig. 9 and *Fig. 10* show the most significant parameters, amplitude and phase of the induced voltage difference.

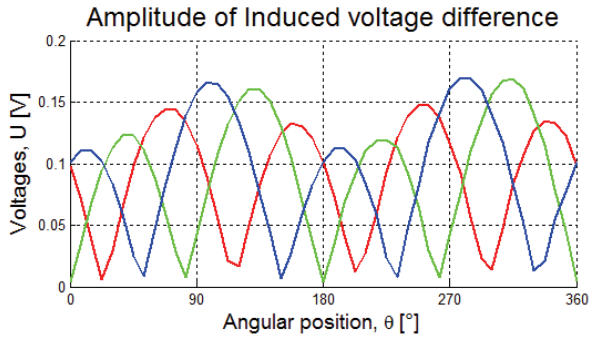

Figure 9: The amplitudes of the induced voltage differencies on the Maxon EC 118890 (red line: Phase 1 excited, green line: Phase 2 excited, blue line: Phase 3 excited)

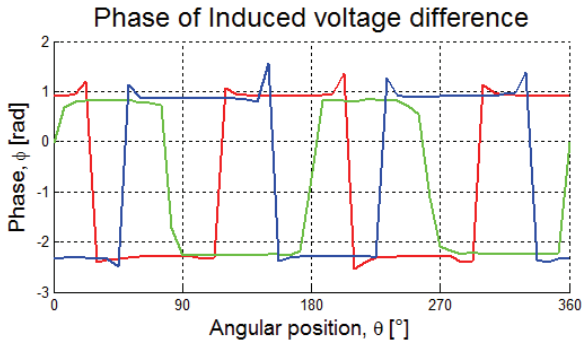

Figure 10: The phases of the induced voltage differencies on the Maxon EC 118890 (red line: Ph. 1 excited, green line: Ph. 2 exc., blue line: Ph. 3 exc.)

[2] MathWorks® and MATLAB® are registered trademarks of the MathWorks, Inc.

Partial position detection method

The phases (Π_i) of the three induced voltage difference signals can be used to coarse position detection. According to Fig. 10, each Π_i has two possible discrete value with π rad difference, and there is six combination of Π_i-s. That makes possible to reduce the rotor position value into two 30° size, opposite sector.

Conclusions

An automated mesurement environment has been implemented for support the development of a sensorless initial position detection method for slotless PMSMs. The analysis of the measured signals discovered measurable anisotropic effect, which depends on the rotor position, but the detected phenomenon has a periodicity of 180°. So an other method is needed to distinguish between the magnet poles to solve the $0 - \pi$ ambiguity problem. In the theoretical part of the work the $\Re_M(\varphi, \Phi)$ radial reluctance function for the rotor magnet should be determined.

ACKNOWLEDGEMENT

We acknowledge the Financial support of this work by the Hungarian State and the European Union under the TÁMOP-4.2.1/B-09/1/KONV-2010-0003 project.

REFERENCES

1. J. PERSSON: Innovative Standstill Position Detection Combined with Sensorless Control of Synchronous Motors, (2005)
2. M. LINKE, R. KENNEL, J. HOLTZ: Sensorless Position Control of Permanent Magnet Synchronous Machines without Limitation at Zero Speed. IEEE 2002, 28th Annual Conference of the Industrial Electronics Society, Vol. 1, (2002) 674–679
3. D. C. HAMILL: Lumped Equivalent Circuits of Magnetic Components: The Gyrator-Capacitor Approach. IEEE Transactions On Power Electronics, 8(2), April, (1993), 97–103